Investigation of Magnetic Field Immunity and Near Magnetic Field Reduction for the Inductors in High Power Density Design

Yanwen Lai and Shuo Wang
Power Electronics and Electrical Power Research Lab
University of Florida
Gainesville, USA
Laiyw124@ufl.edu, shuowang@ieee.org

***Abstract*—This paper investigates the magnetic field immunity and near magnetic field reduction for different inductor winding structures. A novel double-twisted winding structure, which includes two magnetic cores, is proposed for CM inductors. The proposed CM inductor can achieve much lower near magnetic field emission, much better magnetic field immunity against the external magnetic field and much bigger DM impedance than conventional winding structures. Theoretical analysis, magnetic 3D simulations and experiments were conducted to validate the proposed technique.**

Keywords—Near magnetic field emission, winding structure, induced noise voltage, near magnetic field immunity

I. Introduction

The electromagnetic interference (EMI) has become a more and more popular issue when the wide bandgap (WBG) devices are employed in power electronics systems and the switching frequency becomes higher and higher. As one of the most widely used components in power electronics devices, the inductor plays an important role in EMI emission and suppression. On the other hand, to achieve high power density power electronics systems [18], components are very close to each other, which might give rise to EMI issues. The components in limited space might cause interference to each other via near field couplings [6]. For instance, when the current flows through the inductor in the resonant tank of an LLC resonant converter, the inductor can generate significant time varying magnetic field due to the high frequency and high current ripples. The filter inductors of a WBG device powered photovoltaic inverter can also generate significant near magnetic field emissions due to high percentage of high frequency currents. The magnetic field might couple with other components in the systems, which might compromise the operation condition and damage the systems. At the same time, the magnetic inductors can easily pickup stray near magnetic field generated by other components or PCB traces in the systems. The noise voltage will be induced inside the inductors. When the inductors are used for EMI filter components, the induced noise voltages greatly degrade inductor's performance. A stack inductor structure was proposed to mitigate the near magnetic field emission and achieve immunity against external magnetic field interference [3]. Some improved CM choke structures had been developed to achieve better DM impedance performance in [1]- [5]. Both [2] and [3] focus on the inductor near magnetic field radiation reduction but they didn't analyze the induced noise voltages in various inductor structures. The analysis in the reduction of external magnetic field interference had been studied in [3][5]. In [7], the impedance balance concept was proposed to suppress CM noise. Several literature [8]-[12] investigated the parasitic phenomenon within EMI filters. [10] revealed the existence of inductive and capacitive couplings of EMI filters. In [8] the coupling among EMI filter elements could be reduced with self-parasitic cancellation while [9][11] introduced the technique to achieve mutual capacitance cancellation. A technique to improve EMI filter performance by reducing equivalent series inductance and equivalent series resistance was developed in [12]. The application of coupled inductor to DC/DC converters was investigate in [13] to achieve high efficiency. However, it may generate near magnetic field to contaminate other circuits nearby or be susceptible to external magnetic field.

This paper focuses on the investigation of the induced noise voltage in CM and DM inductors due to external magnetic field. Equivalent current loop and circuit are derived to illustrate the generation and cancellation principles of the induced noise voltages in inductors with various winding structures. In section 2, the conventional inductor structures and several improved inductor structures are analyzed and compared within external magnetic field. In section 3, experiments are carried out to verify the analysis in section 2. In section 4, a novel CM inductor is proposed to achieve near magnetic field emission reduction, immunity against the external magnetic field and DM inductance augment. The fundamental principle of near magnetic field emission and noise voltage induction are explored. Simulations are carried out to validate the proposed inductor. In section 5, inductor prototypes are developed, and experiments are conducted to verify the theory and techniques developed in this paper.

II. Induced Noise Voltage dut to External Magnetic Field

A. Inductor with single-ended windings

The single-ended toroid inductor is the most commonly used structure and it has the necessary configuration as an inductor. In this paper, the direction facing towards the incoming line end of the inductor is defined as x direction, the direction facing

towards the inductor side is defined as y direction and z direction is defined to be vertical to the inductor plane, indicated in fig.1 (a). An even magnetic field from arbitrary direction can be decomposed to x, y and z components shown in fig.1 (b).

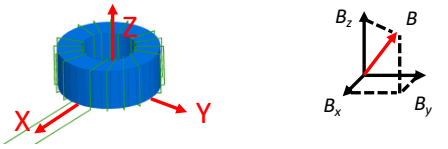

(a) (b)

Fig.1 (a) Definition of x, y and z direction, (b)field components.

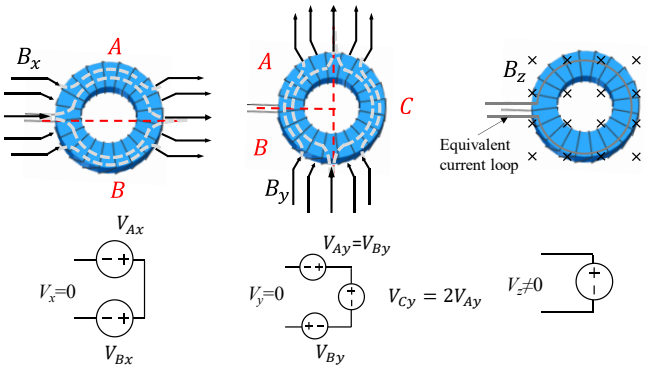

(a) (b) (c)

Fig.2 Equivalent circuit for single-ended winding inductor with(a) x direction field, (b) y direction field, (c) z direction field

When an even time-varying magnetic field propagates along x direction towards a single-ended winding inductor, if applying Faraday's Law to the two halve parts of the winding, A and B, as fig.2 (a) shows, each halve winding is considered to be an induced voltage source. Since the winding structure is symmetrical, the voltages in series on the two separate parts have identical magnitude and they tend to cancel each other. In this case, no noise current is generated. Similarly, when considering the effect of y direction magnetic field, the inductor winding can be viewed as three separate parts as fig.2 (b) shows. The winding turns relationship among the entire winding and the three individual parts can be expressed as

$$N_{total} = N_A + N_B + N_C \tag{1}$$

$$N_A = N_B = \frac{1}{2} N_C \tag{2}$$

where N_{total} is the entire winding turns number and N_A, N_B, N_c are winding turns number of part A, B and C respectively. From equation (1) and (2), the relationship of induced voltages of the three parts can be easily obtained.

$$V = N\frac{A\mathrm{d}B}{\mathrm{d}t} \tag{3}$$

$$V_A + V_B = V_C \tag{4}$$

A is the wire loop area, B is the time-varying magnetic field. As a result, the induced voltages caused by y direction magnetic field cancel each other in the winding. However, the z direction magnetic field induces a noise voltage in the equivalent current loop of the winding as fig.2 (c) shows. In this case, the equivalent current loop can be viewed as a one turn coil and the noise voltage cannot be eliminated. Therefore, the noise current is generated in the winding.

B. Conventional CM inductor with balanced two windings

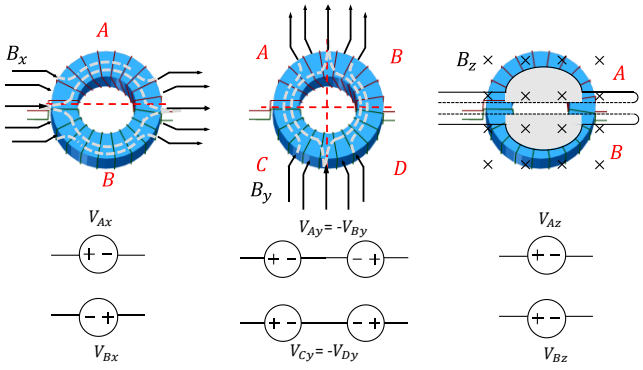

(a) (b) (c)

Fig.3 Equivalent circuit for conventional CM inductor with: (a)x direction field, (b)y direction field, (c)z direction field.

The conventional winding structure gives rise to noise voltage induced by external magnetic field. When a time-varying magnetic field comes along x direction the noise voltage sources can be induced on each winding as fig.3 (a) shows. The noise voltages induced by the magnetic field along y direction can be modeled by considering the two windings to be four separate parts with identical winding turns. The induced noise voltages therefore have identical magnitude and their polarities are shown in fig.3 (b). Since the induced voltages have inverse polarities on each winding, they tend to cancel each other. Besides, it should be noted that the induced noise voltage caused by the magnetic field coming along the z direction depends on the PCB layout or wiring arrangement. If the equivalent wire loop on the PCB has a limited area (shadow area in fig.3 (c)), from equation (3), the induced voltage can be very small. On the contrary, the larger wire loop area gives rise to higher induced voltage magnitude. Dot lines in fig.3 (c) are wiring arrangement on the PCB.

C. DM inductor with balanced two windings

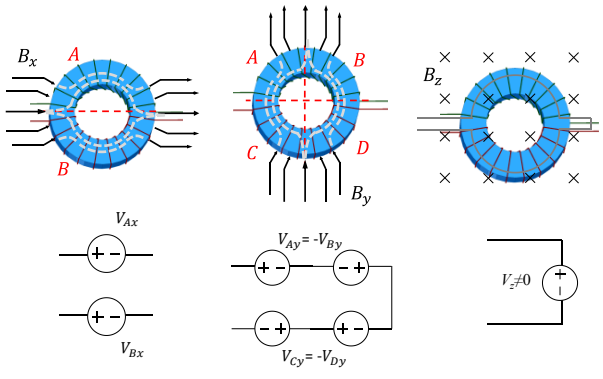

(a) (b) (c)

Fig.4 Balanced two winding DM inductor and its equivalent circuit for induced noise sources due to field, (a) in x direction, (b) in y direction and (c) in z direction.

The balanced two-winding DM inductor can be analyzed similarly. The x direction magnetic field induces one noise voltage on each winding as shown in fig.4 (a). For the y direction field, two voltage sources are generated on each winding in series with inverse polarities so that they could cancel each other shown in fig.4 (b). The z direction field induces a noise voltage on the equivalent current loop shown in fig.4 (c).

D. Inductor with a single twisted winding

The difference between single twisted winding inductor and the single-ended winding inductor is that the wire intersects in the opening window of the single twisted winding inductor. When the time-varying magnetic field comes along x or y direction, a similar analytical procedure can be applied with the conclusion that induced voltages can be eliminated in these two situations, shown in fig.5 (a) and (b). For magnetic field from z direction, induced voltages with the identical magnitude and inverse polarities are generated separately in both current loops and they tend to cancel each in the winding, shown in fig 5 (c). By this way, the induced voltages caused by the magnetic field from x, y and z direction can be eliminated.

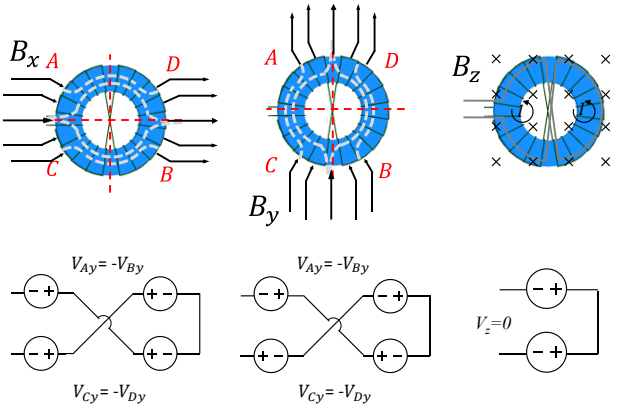

Fig.5 Single twisted winding inductor and its equivalent induced noised circuit in (a)x direction, (b)y direction and (c)z direction.

E. DM inductor with balanced twisted windings

The structure of the balanced twisted windings DM inductor is shown in fig.6. When it is conducting DM current, the two windings are positive coupled to generate great DM impedance when conducting DM current. The induced voltages caused by the magnetic fields from x, y and z directions can be derived in similar analytical procedure and the equivalent circuits are shown in fig 7. For the situations that the magnetic fields come along x and y direction, the induced noise voltages on one winding can be canceled by each other.

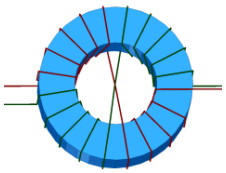

Fig.6 Balanced twisted windings DM inductor

Moreover, the z direction magnetic field also induces inverse polarity noise voltages in the two current loops. In conclusion, the balanced twisted windings DM inductor has immunity against external magnetic field from all directions.

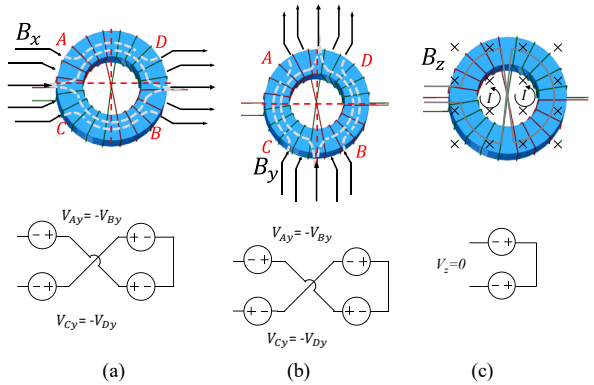

Fig.7 Balanced twisted windings DM inductor and its equivalent induced noised circuit in (a)x direction, (b)y direction and (c)z direction.

F. CM inductor with balanced twisted windings

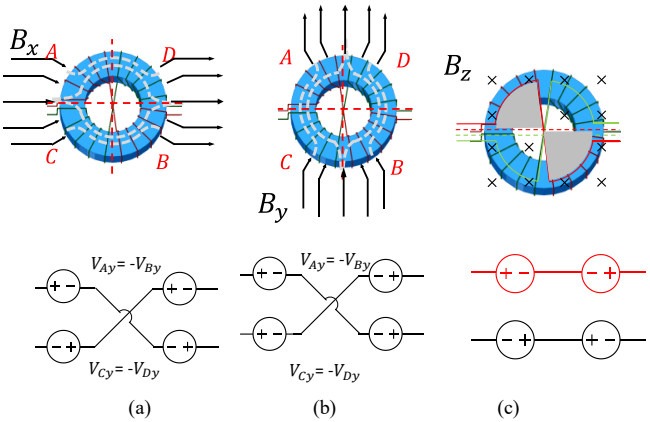

Fig.8 Balanced twisted windings CM inductor current loops and its equivalent induced noised circuit in (a)x direction, (b)y direction and (c)z direction.

The difference between the conventional balanced two winding CM inductor and the balanced twisted windings CM inductor is the wire twisted arrangement in the inductor opening window. The noise voltages generated in balanced twisted windings CM inductor by x and y direction magnetic field can be derived, shown in fig.8 (a) and (b). It should be noted that the PCB layout still affects the induced voltages caused by z direction magnetic field. In fig.8 (c), for instance, if the two sector areas (shadow area) of the red winding have identical area, inverse voltages will be induced on quarter windings with

TABLE I
MAGNETIC FIELD IMMUNITY OF VARIOUS INDUCTORS

Noise cancellation / Structure types	X direction	Y direction	Z direction
Single-ended winding inductor	Yes	Yes	No
Single twisted winding inductor	Yes	Yes	Yes
Balanced two-winding CM inductor	No	Yes	Depending on PCB layout
Balanced twisted windings CM inductor	Yes	Yes	Depending on PCB layout
Balanced two-winding DM inductor	No	Yes	No
Balanced twisted windings DM inductor	Yes	Yes	Yes

identical magnitude so that they can cancel each other. In another way, if the shadow area is designed to be small, the induced voltage magnitude could be small as well.

Table I is to summarize the external magnetic field immunity of the inductor structures analyzed above. It should be noticed that the twisted winding structures are showing better immunity property. Experiments are carried out in next section to verify the previous analysis.

III. Experimental Verification for Induced Voltage Analysis

In this section, the analysis of induced noise caused by external magnetic field in inductor structures analyzed in section II is validated with experiments.

The inductor structures in section II are built with powder cores with relative permeability of 5000. The model number is 35T1000-00H from Laird-Signal Integrity Products. The inner diameter is 14.23mm and the outer diameter is 26.67mm. Core height is 11mm. The turns number for both single winding inductors and two-winding inductors is 24. All the inductors have identical dimensions and turns number to keep the inductance identical. The inductance of inductors with single winding structures is $2.67mH$. The CM inductance of CM inductors with two winding structure is $637\ \mu H$ and the DM inductance of DM inductors with two winding structure is $2.67mH$. AWG #26 wire is used for all inductors.

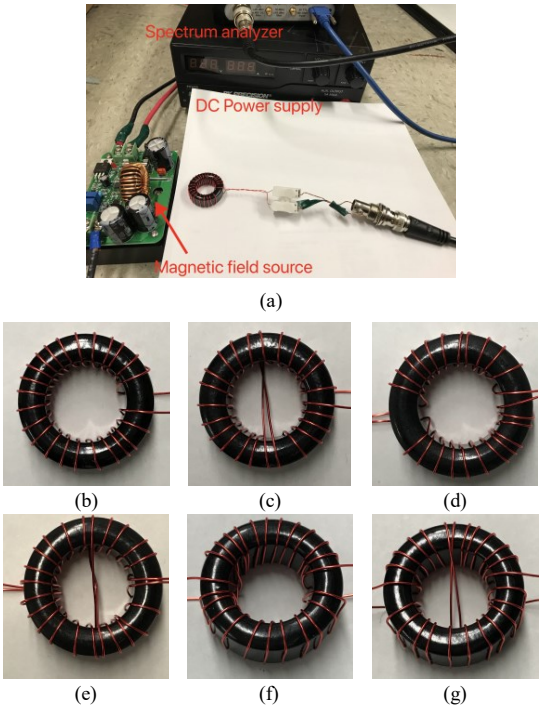

Fig. 9 (a)Experiment set up, (b)single-ended winding inductor, (c)single twisted winding inductor, (d)balanced two winding CM inductor, (e)balanced twisted windings CM inductor, (f)balanced two winding DM inductor, (g)balanced twisted windings DM inductor.

A DC-DC 600W boost Converter from Shenzhen Geree Electronics Co., Ltd is used for magnetic field source, with the input voltage 30V and input current 11.5A. The DC voltage source is Switching DC Power Supplies Discontinued Model 1902 from BK PRECISION. A 4.7Ω resistor is used for load. All the inductors were measured at the distance of 30mm from the converter. A RSA306B REAL-TIME SPECTRUM ANALYZER from Tektronix was used for measuring both CM and DM noise spectra in the inductors. To measure the CM noise, the inductor windings were connected in parallel. To measure the DM noise, the inductor windings were connected in series. Experiment set up and inductor prototypes are shown in fig. 9.

Fig.10 shows the measurement result for the single winding structure inductor where the inductor with twisted winding structure has approximately 20dB reduction compared with that without twisted winding structure. For the two windings CM inductors, the twisted structure compared with the not twisted structure has 20dB reduction for both CM and DM noise as shown in fig.11 (a) and (b). For the two winding DM inductors, the twisted structure compared with the structure not twisted has 33dB and 20dB reduction for CM and DM noise respectively as shown in fig.12 (a) and (b).

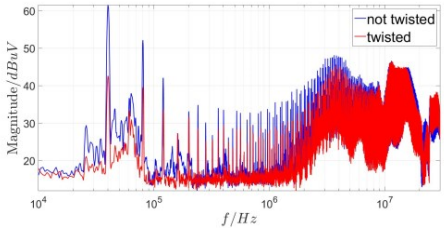

Fig. 10 Noise spectra for single winding inductors

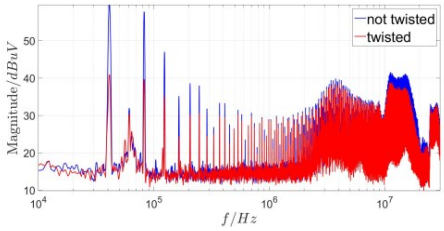

(a)

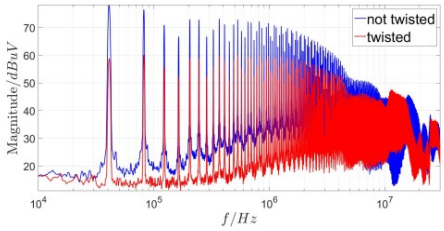

(b)

Fig. 11 Noise spectra for two winding CM inductors: (a)CM noise, (b)DM noise

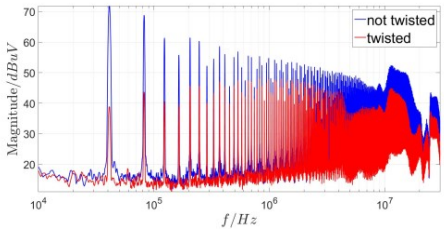

(a)

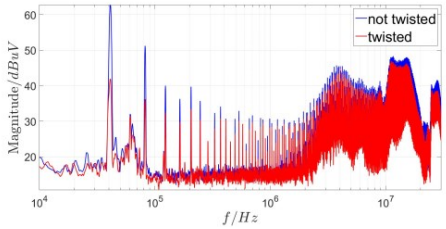

(b)

Fig. 12 Noise spectra for two winding DM inductors: (a)CM noise, (b)DM noise

In conclusion, the twisted technique can lower the induced noise magnitude by at least 20dB and up to 33dB in the inductor core.

IV. Proposed CM Inductor Structure to Reduce Induced Voltage and Emitted Near Magnetic Field

As [2] and the previous section analyzed, the balanced two winding CM or DM inductor generates great near magnetic field radiation when conducting DM or CM current respectively and noise voltages will be induced by external magnetic field due to their winding structures. One approach to reduce near magnetic field is to twist the windings in the canter of the inductor open windows. However, leakage flux of the inductors, in the form of near magnetic field emission, provides DM inductance for CM inductor or CM inductance for DM inductor. The suppression of near magnetic field emission gives rise to the reduction in DM/CM inductance of CM/DM inductor if the twisted winding technique is applied. Although the twisted winding technique is useful in near magnetic field emission suppression, the reduction in DM/CM inductance for CM/DM inductor is not expected. A KEYSIGHT impedance analyzer is used to measure the inductance of the inductors and the results are shown in Table II. The DM inductance for balanced twisted windings CM inductor is lower than that of the balanced conventional CM inductor and the CM inductance for balanced twisted windings DM inductor is also lower than that of the balanced two winding DM inductor, which verify the previous analysis.

TABLE II
Inductors Inductance

Structure types	CM inductance	DM inductance
Single-ended winding inductor	-	2.67mH
Single twisted winding inductor	-	2.67mH
Balanced two winding CM inductor	637 μH	**6.37 μH**
Balanced twisted windings CM inductor	637 μH	**2.07 μH**
Balanced two winding DM inductor	**1.51 μH**	2.67mH
Balanced twisted windings DM inductor	**0.65 μH**	2.67mH

In this section, a new CM inductor structure is proposed to achieve near magnetic field radiation reduction, DM inductance augment and external magnetic field immunity. The proposed inductor is including two cores. Core A with smaller size is placed in the open window of core B. The winding arrangement is show in fig.14.

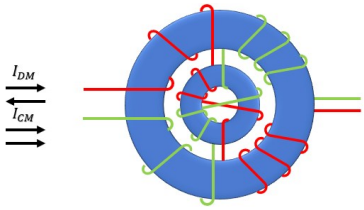

Fig.13 Proposed CM inductor

From fig.13, the configuration of the proposed structure can be defined as double twisted two winding structure since each of core A and B has a twisted two winding CM inductor structure. The proposed inductor is entirely symmetrical in structure. To achieve external magnetic field immunity, identical winding turns number should be assigned to every 90° span on each core respectively. Therefore, the winding turns number should be a multiple of four.

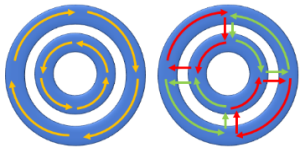

(a) (b)

Fig. 14 Proposed CM inductor magnetic flux conducting (a)CM current, (b)DM current

When CM current is conducted, most of the magnetic flux is confined within the high permeability cores as fig.14 (a) shows, which can provide CM impedance as the conventional CM inductor. When DM current is conducted, the magnetic flux in both cores flows as fig.14 (b) shows. In this case, leakage flux of the cores goes through the high permeability core magnetic paths instead of air, confining leakage flux within the inductor cores to increase DM impedance and reduce near magnetic field radiation simultaneously. Moreover, the leakage fluxes in air generated by each core are in reversed polarities so that they can cancel each other.

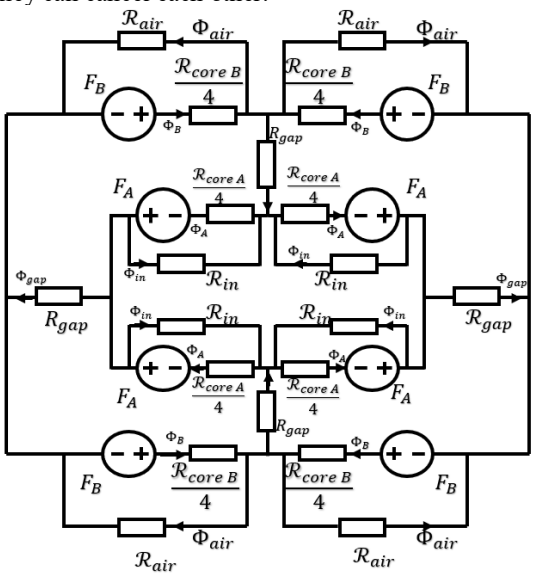

Fig. 15 Magnetic circuit for the proposed CM inductor

The composed proposed structure and its equivalent magnetic circuit can be therefore derived for further investigation. In the magnetic circuit shown in fig.15, F_A and F_B represent the MMF generated by the quarter section of the cores respectively. ϕ_A and ϕ_B represent the magnetic flux flowing through the cores restively. $\mathcal{R}_{core\,A}$ and $\mathcal{R}_{core\,B}$ represent the reluctance of the entire cores respectively. $\mathcal{R}_{in}$ represents the reluctance of air in the open window of core A and ϕ_{in} represents the flux flowing through it. $\mathcal{R}_{air}$ represents the reluctance of air in space around the core B and ϕ_{air} represents the magnetic flux flowing through it. $\mathcal{R}_{gap}$ represents the equivalent reluctance of the air gap between the two cores and ϕ_{gap} represents the flux flowing through it. Because of the symmetry of the proposed inductor, the magnetic circuit in fig.15 can be further simplified to fig.16 for calculation propose.

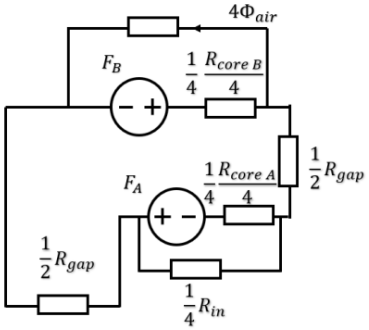

Fig. 16 Simplified magnetic circuit for proposed CM inductor

Since the ϕ_{air} represents the near magnetic field radiation from the proposed CM inductor with DM current excitation, the near magnetic field radiation can be eliminated if ϕ_{air} is greatly reduced.

Assumption is made as

$$\mathcal{R}_{core\,A}, \mathcal{R}_{core\,B} < \mathcal{R}_{gap} \ll \mathcal{R}_{air}, \mathcal{R}_{in} \tag{5}$$

Base on fig.14, ϕ_{air} can be derived as

$$4\phi_{air} \approx \frac{F_B\left(\mathcal{R}_{gap} + \frac{\mathcal{R}_{core\,A}}{16}\right) - F_A\frac{\mathcal{R}_{core\,B}}{16}}{(\mathcal{R}_{gap} + \frac{\mathcal{R}_{core\,A}}{16} + \frac{\mathcal{R}_{core\,B}}{16}) \times \frac{1}{4}\mathcal{R}_{air}} \tag{6}$$

From (6), the elimination can be achieved if ϕ_{air} reduces to zero. Then the elimination condition can be derived as

$$\frac{F_B}{F_A} = \frac{N_B}{N_A} = \frac{\frac{\mathcal{R}_{core\,B}}{16}}{\mathcal{R}_{gap} + \frac{\mathcal{R}_{core\,A}}{16}} \tag{7}$$

In (7), N_A and N_B represent the winding turns number on core A and B respectively. The ϕ_{in} has inverse direction in space compared with ϕ_{air} so they tend to cancel each other. It should also be noted that the ϕ_{in} is considered to have little contribution to the near magnetic field radiation since it is confined in the center of core A.

Several conditions should be satisfied to design a proposed CM inductor with specific inductance L_{CM}, When conducting CM current, the mutual inductance between core A and B is ignored as most of the magnetic flux is confined within the cores.

$$L_{CM} = \frac{{N_A}^2}{\mathcal{R}_{core\,A}} + \frac{{N_B}^2}{\mathcal{R}_{core\,B}} \tag{8}$$

$$\mathcal{R}_{core\,A} = \frac{l_A}{\mu_0\mu_A A_A} \tag{9}$$

$$\mathcal{R}_{core\,B} = \frac{l_B}{\mu_0\mu_B A_B} \tag{10}$$

$$\mathcal{R}_{gap} = \frac{l_{gap}}{\mu_0 A_{gap}} \approx \frac{r_B - R_A}{\mu_0 A_{gap}} \tag{11}$$

$$A_{gap} \approx \frac{\pi(r_B + R_A)(H_B + H_A)}{16} \tag{12}$$

In the equations, l_A and l_B represent the effective length of core A and B respectively. μ_A and μ_B represent the relative permeability of core A and B respectively. μ_0 is the vacuum permeability. The r_B represents the inner radius of core B and the R_A represents the outer radius of core A. The $\mathcal{R}_{core\,A}$ and $\mathcal{R}_{core\,B}$ represent the reluctance of core A and B. The l_{gap} represents the equivalent length of the air gap between core A and B and it can be approximately equal to the difference between r_B and R_A. In (11), H_B and H_A represent the height of the two cores. In (12), the A_{gap} represents the equivalent cross-sectional area of the magnetic flux ϕ_{gap}. It is approximately equal to $\frac{1}{8}$ cross-sectional area of the whole air gap between the two cores. The fringing effect is ignored since the difference between H_B and H_A, r_B and R_A is assumed to be limited.

From equation (7), it indicates that the MMF in core B should be lower than that in core A, which means that the wiring turns on outer core should be less than that on the inner core. Also, if the parameters of the cores are modified to strictly meet the numeric relationship between turns number and inductor reluctance as equation (7) shows, the proposed structure can therefore be further optimized. Table III includes the

TABLE III
INDUCTOR PARAMETERS

Inductor structure	Core	Outer diameter	Inner diameter	Height	Turns number	μ_r
Conventional structure	B	26.67mm	14.23mm	11mm	22	5000
Proposed structure	A B	12.50mm 26.67mm	7.50mm 14.23mm	5.95mm 11mm	24 20	2200 5000
Optimized proposed structure	A B	12.50mm 26.90mm	7.50mm 14.50mm	5.95mm 11.1mm	48 20	2200 14

parameters for conventional structure, proposed structures before and after optimized. All the inductors were designed to obtain identical CM inductance $L_{CM} = 637\mu H$. All three inductors satisfy equation (8). The optimized proposed inductor also satisfies (7) when proposed inductor does not. Fig.17 shows the simulation results which are measured at the distance of 25mm from the top of the inductors. It can be found that both proposed and optimized proposed inductors can significantly reduce near magnetic emission compared with the conventional structure inductor. The optimized proposed inductor can further

reduce the near magnetic field emission compared with the proposed structure.

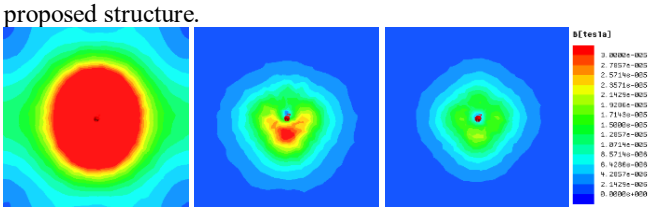

(a) (b) (c)

Fig. 17 Near field emission simulation for (a) conventional CM inductor, (b) proposed CM inductor and (c) optimized proposed CM inductor

V. Experiment Verification for the Porposed Inductor

A. *Induced noise measurement*

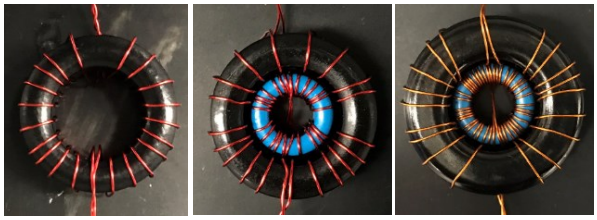

(a) (b) (c)

Fig.18 Prototypes for (a) conventional CM inductor, (b) proposed CM inductor, (c)optimized proposed CM inductor

Three inductor prototypes, shown in fig.18, were built referring to the parameters in Table III. AWG #26 is used for conventional and proposed inductor structure, and AWG #28 is used for the optimized proposed structure inductor. The measurement was also carried out with experiment set up shown in fig.9 (a) and the results are shown in fig. 19.

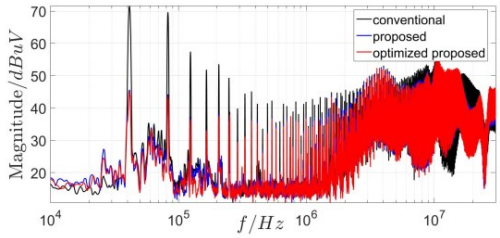

(a)

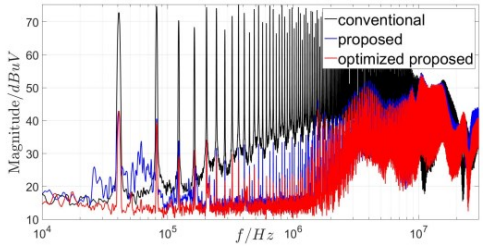

(b)

Fig. 19 Noise spectra for three CM inductor structures (a)CM noise, (b)DM noise

For both CM and DM induced noise, the proposed and optimized proposed structure have similar magnitudes levels. Compare with the noise magnitude of conventional structure, the proposed structures reduce the CM noise magnitude by 26dB at low frequency and lower the DM noise by up to 63dB within a wide frequency scale.

B. *Near Field Measurement*

The near magnetic field was measured with a signal generator RIGOL DG4062, a Beehive Electronics 100C EMC probe, an Amplifier Research Model 25A250A amplifier and a Rohde & Schwarz FSH4 spectrum analyzer. A 200kHz sinusoidal voltage was applied to the measured inductors and the DM current conducted was controlled to be maintained at 1A, monitored by a current clamp connected to a RIGAL DE1052E digital oscilloscope. The experiment set up is shown in fig.20. There were 7*7=49 measurement points on the coordinate board and the entire measurement area is 20cm*20cm.

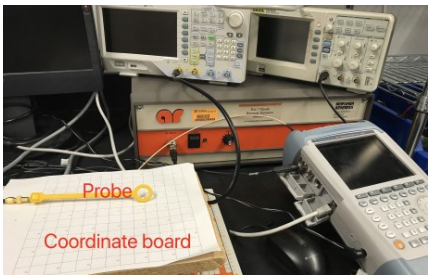

Fig.20 Near magnetic field experiment set up

The measured inductor is placed under the coordinate board and the EMC probe was adjusted to measure the magnetic field in x, y, and z direction at each measurement point. Then the measurement data was exported from the spectrum analyzer to calculate the composite magnetic field density according to equation (13),

$$B = \sqrt{{B_x}^2 + {B_y}^2 + {B_z}^2} \quad (13)$$

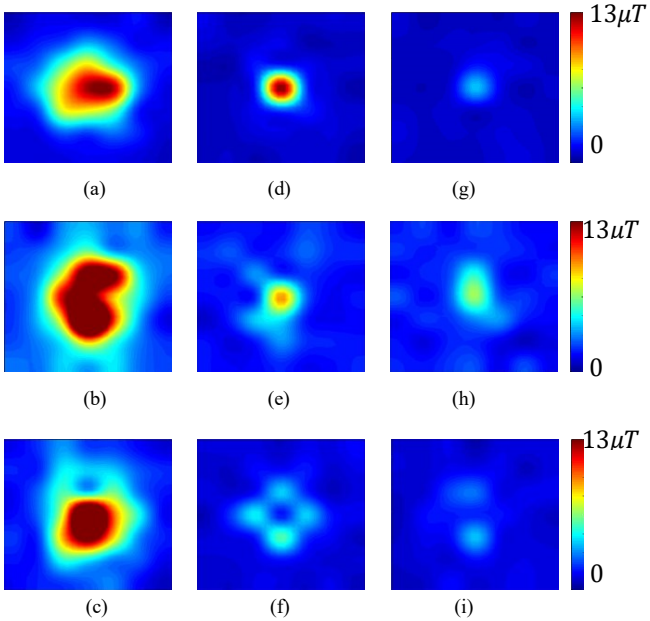

(a) (d) (g)

(b) (e) (h)

(c) (f) (i)

Fig.21 Measured near magnetic field emission of conventional inductor measured in (a)x direction, (b)y direction, (c)z direction; measured near field of proposed inductor in (d)x direction, (e)y direction, (f)z direction and measured near field of optimized proposed inductor in (g)x direction, (h)y direction, (i)z direction.

The measurement was carried out at the distance of 25mm from the inductor from x, y and z direction defined in the previous section. The measurement results are shown in fig.21. As the figure shows, the near magnetic field emission of proposed and optimized proposed structure can be significantly reduced compared with that of the conventional inductor from all directions. Besides, the optimized proposed inductor has even lower near magnetic field emission than the proposed structure. The experiment results verify the analysis in previous sections.

C. Impedance Measurement

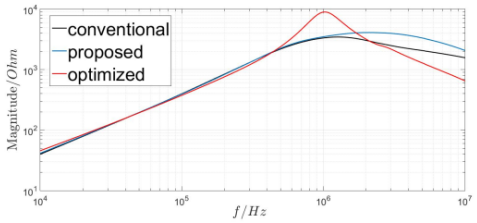

(a)

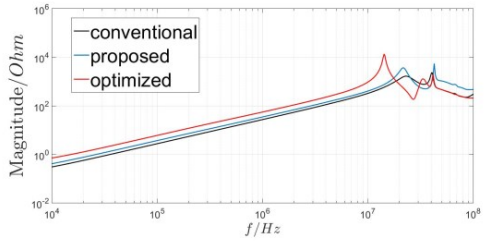

(b)

Fig.22 Impedance of inductors (a) CM impedance, (b) DM impedance

The impedance of the inductors was measured with a KEYSIGHT impedance analyzer. The inductors are all designed to have identical CM impedance as fig.22 shows. At low frequency the inductance is $L_{CM} = 637\mu H$. The DM inductance for the conventional inductor, proposed inductor and optimized proposed inductor are 4.3 μH, 5.9 μH and 9.7 μH respectively.

VI. Conclusion

In this paper, the induced noise voltage in inductors due to external near magnetic field is investigated. The generation of induced noise voltage in different inductors are analyzed and summarized, and equivalent circuits are developed. Experiments are carried out to verify the analysis. A novel CM inductor with two cores is proposed to achieve near magnetic field emission reduction, immunity against the external magnetic field and DM inductance augment. Furthermore, the optimization technique for the reduction of the emitted near magnetic field from the proposed inductor is investigated and simulations validated the developed technique. The prototypes are developed and experiments are carried out to validate the analysis.

Acknowledgement

Micrometal, Inc. offered inductor samples for experiments.

Referrence

[1] R. Lai, Y. Maillet, F. Wang, S. Wang, R. Burgos and D. Boroyevich, "An Integrated EMI Choke for Differential-Mode and Common-Mode Noise Suppression," in IEEE Transactions on Power Electronics, vol. 25, no. 3, pp. 539-544, March 2010.

[2] B. Zhang and S. Wang, "Analysis and reduction of the near magnetic field radiation from magnetic inductors," 2017 IEEE Applied Power Electronics Conference and Exposition (APEC), Tampa, FL, 2017, pp. 2494-2501.

[3] Y. Chu, S. Wang, N. Zhang and D. Fu, "A Common Mode Inductor With External Magnetic Field Immunity, Low-Magnetic Field Emission, and High-Differential Mode Inductance," in IEEE Transactions on Power Electronics, vol. 30, no. 12, pp. 6684-6694, Dec. 2015.

[4] W. Tan, C. Cuellar, X. Margueron and N. Idir, "A Common-Mode Choke Using Toroid-EQ Mixed Structure," in IEEE Transactions on Power Electronics, vol. 28, no. 1, pp. 31-35, Jan. 2013.

[5] Y. Chu, S. Wang, J. Xu and D. Fu, "EMI reduction with near field coupling suppression techniques for planar transformers and CM chokes in switching-mode power converters," 2013 IEEE Energy Conversion Congress and Exposition, Denver, CO, 2013, pp. 3679-3686.

[6] Shuo Wang, F. C. Lee and W. G. Odendaal, "Using scattering parameters to characterize EMI filters," *2004 IEEE 35th Annual Power Electronics Specialists Conference (IEEE Cat. No.04CH37551)*, 2004, pp. 297-303 Vol.1.

[7] S. Wang, P. Kong and F. C. Lee, "Common mode noise reduction for boost converters using general balance technique," 2006 37th IEEE Power Electronics Specialists Conference, Jeju, 2006, pp. 1-6.

[8] S. Wang, R. Chen, J.D. Van Wyk, F. C. Lee, W.G. Odendaal, "Developing parasitic cancellation technologies to improve EMI filter performance for switching mode power supplies", Electromagnetic Compatibility IEEE Transactions on, vol. 47, pp. 921-929, 2005, ISSN 0018-9375.

[9] S. Wang, F. C. Lee, J. D. van Wyk, "Design of Inductor Winding Capacitance Cancellation for EMI Suppression", Power Electronics IEEE Transactions on, vol. 21, pp. 1825-1832, 2006, ISSN 0885-8993.

[10] S. Wang, F.C. Lee, Dan. Y. Chen, W. G. Odendaal, "Effects of Parasitic Parameters on EMI Filter Performance", IEEE Transactions on Power Electronics, Vol. 19, No. 3, May 2004

[11] S. Wang, F. C. Lee and J.D. van Wyk, "Inductor Winding Capacitance Cancellation Using Mutual Capacitance Concept for Noise Reduction Application," Electromagnetic Compatibility, IEEE Transactions, Volume 48, Issue 2, May, 2006, pp. 311-318.

[12] S. Wang, F. C. Lee and W. G. Odendaal, "Cancellation of Capacitor Parasitic Parameters for Noise Reduction Application," Power Electronics, IEEE Transactions, July, 2006, pp. 1125-1132.

[13] F. S. F. Silva et al., "High gain DC-DC boost converter with a coupling inductor," 2009 Brazilian Power Electronics Conference, Bonito-Mato Grosso do Sul, 2009, pp. 486-492.

[14] H. Zhang, B. Zhang and S. Wang, "Integrated common mode and differential mode inductors with low near magnetic field emission," 2017 IEEE Energy Conversion Congress and Exposition (ECCE), Cincinnati, OH, USA, 2017, pp. 5375-5382.

[15] H. Zhang, S. Wang and Q. Wang, "Winding and air gap configurations for power inductors to reduce near magnetic field emission," 2017 IEEE Energy Conversion Congress and Exposition (ECCE), Cincinnati, OH, USA, 2017, pp. 903-910.

[16] M. J. Nave, "On modeling the common mode inductor," IEEE 1991 International Symposium on Electromagnetic Compatibility, Cherry Hill, NJ, 1991, pp. 452-457.

[17] D. J. Wilcox, M. Conlon and W. G. Hurley, "Calculation of self and mutual impedances for coils on ferromagnetic cores," in IEE Proceedings A - Physical Science, Measurement and Instrumentation, Management and Education - Reviews, vol. 135, no. 7, pp. 470-476, September 1988.

[18] F. C. Lee, J. D. van Wyk, Z. X. Liang, R. Chen, S. Wang and B. Lu, "An integrated power electronics modular approach: concept and implementation," *The 4th International Power Electronics and Motion Control Conference, 2004. IPEMC 2004.*, Xi'an, 2004, pp. 1-13 Vol.1.